Diffuse reflectance UV-visible spectroscopy for the qualitative and quantitative study of chromophores adsorbed or grafted on silica

Sylvie Lacombe-Lhoste, H. Cardy, N. Soggiu, Sylvie Blanc, J.L. Habib-Jiwan, J.Ph. Soumillion

ELSEVIER SCIENCE B.V. [DTD 4.2.0]
JOURNAL MICMAT ARTICLE No. 1034
PAGES 01-17 DISPATCH 28 May 2001
MICMAT 1034
PROD. TYPE: FROM Disk
A

ELSEVIER

MICROPOROUS AND MESOPOROUS MATERIALS

Microporous and Mesoporous Materials 000 (2001) 000–000

www.elsevier.nl/locate/micromeso

Diffuse reflectance UV–Visible spectroscopy for the qualitative and quantitative study of chromophores adsorbed or grafted on silica

S. Lacombe [a,*], H. Cardy [a], N. Soggiu [a], S. Blanc [a], J.L. Habib-Jiwan [b], J.Ph. Soumillion [b]

[a] *UMR CNRS 5624, Université de Pau, CURS, BP1155, 64013 Pau Cedex, France*
[b] *Unité de Chimie des matériaux (CMAT), Photochimie, Université Catholique de Louvain, Place Louis Pasteur, 1, B1348 Louvain la Neuve, Belgium*

Received 23 February 2001; received in revised form 4 May 2001; accepted 7 May 2001

Abstract

Diffuse reflectance UV–Visible spectroscopy (DRUV) is used to study the adsorption and grafting of the pyrene derivative **1** on different types of silicas. For the adsorbed silicas, the formation of dimeric aggregates is evidenced both by DRUV and by fluorescence spectroscopy. The processing of the UV spectrophotometric data allows, as in solution, the determination of apparent equilibrium constants and of the spectra of the dimer. From these results, two sets of silicas are distinguished according to the amount of dimer formed and to its UV spectrum. Lower amounts of dimeric species are found on silica with either large pore size or low particle size. The spectrum in this case is only slightly red-shifted relative to that of the monomeric compound. When the pore size decreases, dimer formation is more significant and its spectrum is more characteristic. The results obtained for adsorbed silicas were quantitatively treated and the Kubelka–Munk function, $F(R)$, plotted against the concentration. Attempts to estimate the loading of silicas grafted with **1** were undertaken. It appears that small particle size silica gives rise to the highest loading and to the best quality DRUV spectra as a consequence of a minor amount of fluorescent dimer. On the other hand, it is shown that the loading of grafted silica is difficult to control by the used grafting process and that milder conditions are required. © 2001 Published by Elsevier Science B.V.

Keywords: Silica; Adsorption; Grafting; Diffuse reflectance UV–Visible spectroscopy

1. Introduction

Grafted silicas are commonly used in different areas such as specific chromatographic separations, hetrogeneous catalysis [1] or heterogeneous photosensitization [2]. The characteristics of the grafted silicas are of utmost importance for these applications. In the particular case of photochemical reactions, a good knowledge of the supported photosensitizer concentration is required, besides the important parameters of the silica itself: specific surface area, size of the pores and of the particles. Microanalysis is most often used for

* Corresponding author. Tel.: +33-5-5992-3078; fax: +33-5-5980-8344.
E-mail address: sylvie.lacombe@univ-pau.fr (S. Lacombe).

1387-1811/01/$ - see front matter © 2001 Published by Elsevier Science B.V.
PII: S1387-1811(01)00315-8

this goal. However, when working with weakly loaded silicas, discrepancies are observed between the results obtained from the different analyzed elements [3]. In some cases, specific chemical analysis may be achieved like for instance acido basic titrations [4]. More recently, solid state ^{13}C and ^{29}Si-NMR [5,6] has allowed the determination of the grafting yields of various functionalized silicas. Quantitative determination of the grafting ratios can also be made by diffuse reflectance infrared spectroscopy (DRIFT) [7–9].

Diffuse reflectance UV–Visible spectroscopy (DRUV) has been most often considered as a tool for the qualitative characterization of supported catalysts [10–14] or modified zeolites [15–17]. Few quantitative analyses have been performed with this method [18,19], although they could be possible using the Kubelka–Munk remission function [20].

In this work, the use of DRUV spectroscopy aimed to measure the loading of silica powders grafted with organic chromophores has been studied. Pyrene-grafted silicas were chosen due to their easy synthesis and to their characteristic absorption and emission spectra. In a preliminary step, the triethoxysilyl derivative **1** is simply adsorbed on different silica-gels. The DRUV spectra of these adsorbed solids are collected as the basis data set for a calibration curve used for the estimation of the loading of the grafted silicas. During the adsorption study, the influence of the pore and particle size on the spectroscopic behavior of adsorbed chromophore has been assessed. The fluorescence spectroscopy of the adsorbed samples has been used to evaluate possible excimer formation [21,22].

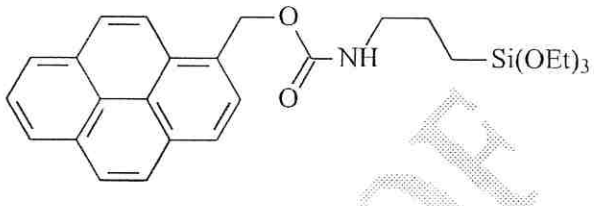

2. Experimental

The silica gels were purchased from Aldrich or from Fluka (Table 1) and were used for adsorption after drying 12 h at 100°C in an oven. Toluene was dried over sodium and stored on molecular sieves. The triethoxysilyl precursor **1** and the different grafted silicas were prepared according to reported methods. Toluene was used instead of DMF for the grafting of the silicas [22].

2.1. Preparation of the calibration samples

Adsorbed samples are usually prepared by mixing the inorganic support with a solution of the chromophore followed by a slow evaporation of the solvent [19,23]. In order to avoid the formation of crystallites on the surface and to mimic the adsorption step occurring at the beginning of a grafting process, an alternative method has been used in this work. Solutions of **1** in toluene at known concentrations are prepared. A known amount of dry silica is then introduced, and the mixture is placed on a stirring orbital table for 1 h at room temperature. The silica is then filtered under vacuum on a porous glass and dried in an oven under vacuum at 100°C. The amount of adsorbed compound is deduced by UV spectroscopy, from the difference between the chromophore concentrations in the solvent before and after adsorption.

Table 1
Characteristics of the silicagels used in the study

Notation	Particle size (μm)	Specific surface area (m^2/g)	Pore size (Å)	Origin and commercial reference
Sil100	63–210	300	100	Aldrich 40,360-1
Sil60-1	63–210	500	60	Aldrich 28,862-4
Sil40	63–210	750	40	Aldrich 40,356-3
Sil60-2	<63	500	60	Fluka 60739

2.2. DRUV and fluorescence spectroscopy

DRUV measurements were made on a Varian Cary 5 Spectrometer equipped with a Praying Mantis (Harrick Scientific Corporation). For each silica, several measurements were made and a mean value of the reflectance ($\%R$) was used in order to take into account the problems arising from a possible inhomogeneity of the surface. The UV range is limited to 250 nm on the high energy side by the absorption of silica in this region. The spectra are displayed in $F(R)$ Kubelka–Munk units, with:

$$F(R) = \frac{(1-R)^2}{2R} = \frac{k}{S} \quad (1)$$

where k and S are the absorption and scattering coefficients [24]. This equation only applies to optically thick samples for which any further increase of the thickness does not affect the experimentally determined reflectance. For an ideal diffuser, the reflected radiation has the same intensity in all the directions.

In the absence of intermolecular interactions or if these interactions are constant, i.e. at low concentrations

$$k = \varepsilon C \quad (2)$$

where ε and C denote, respectively, the molar extinction coefficient and the concentration of the adsorbate. A linear relation for the remission function $F(R)$ as a function of the concentration of the adsorbate is expected, provided that the scattering coefficient S remains the same and therefore that the same type of silica is used for the blank spectrum as for the other samples (especially regarding the particle size).

If intermolecular interactions occur

$$k = \sum_i \varepsilon_i C_i \quad (3)$$

where the summation refers to the possible presence of different species (monomer, dimers, aggregates, etc.).

Due to the definition of the Kubelka–Munk function (Eq. (1)), values greater than 25 cannot be used because reflected light R is less than 1% at this level and a bad detector response is expected.

In order to obtain quantitative information on the dimerization process (apparent dimerization equilibrium constant and adsorption coefficients for monomer and dimer species), the spectrophotometric data are processed with the Letagrop–Spefo program which uses the Newton–Raphson algorithm to solve mass balance equations and a pit-mapping method to minimize the errors and to determine the best parameter values [25–29]. Fluorescence spectra of the powdered samples were measured on the dried powder and in front surface on a SLM Aminco 48000S spectrofluorimeter working in the ratio mode and with an excitation wavelength at 340 nm.

3. Results

Different types of silica (Table 1) have been used in order to evaluate the influence of the specific surface area (related to the pore size) and of the particle size, on the spectroscopic features of adsorbed **1** and on the grafting yields.

3.1. DRUV and fluorescence study of adsorbed 1

The DRUV spectra obtained for Sil60-1 are given in Fig. 1a. In Fig. 1b, the same spectra have been normalized on the most intense band at 337 nm. In Fig. 2 scaled spectra are given for the other silicas. The normalization of the spectra allows one to evidence the formation of aggregates related to band shape deformation or broadening.

The scaled spectra displayed in Fig. 1b for Sil60-1 and in Fig. 2 for the other silicas deserve the following comments:

- The spectrum of adsorbed pyrene is close to its spectrum in solution with a slight hypsochromic shift (Fig. 3).
- A distorsion of the scaled spectra may be observed at high concentrations, i.e. in the range 4.5–8.9 μmol/g for Sil60-1: the 337 nm band broadens on the low energy side, while the relative intensities of the 322 and 308 nm bands on the high energy side increase. At the same time, the intensity variation of the band at 262 nm is less straightforward. Although very characteris-

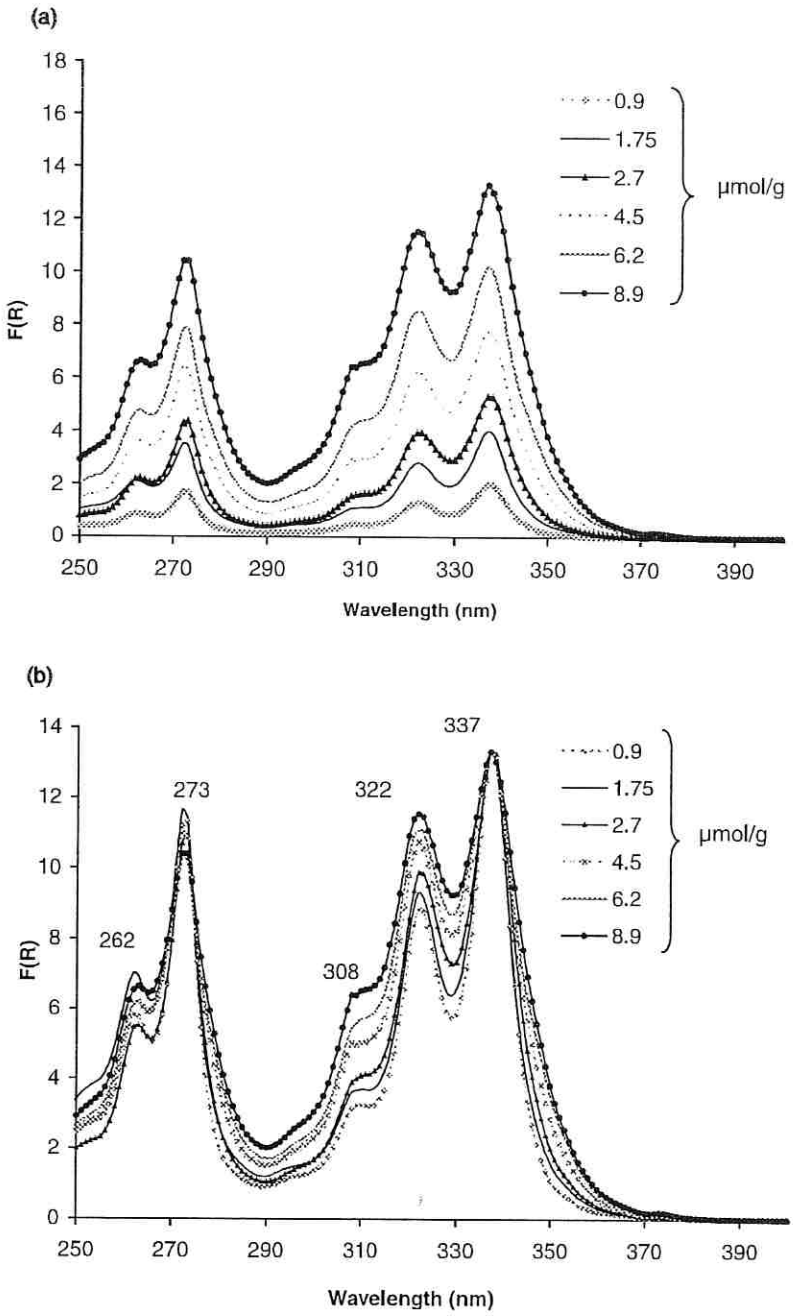

Fig. 1. DRUV spectra of the pyrene derivative **1** adsorbed on Sil60-1 at different concentrations. (a) Unormalized spectra. (b) Spectra normalized on the intensity of the 337 nm band.

tic for Sil60-1 (Fig. 1b), Sil100 (Fig. 2a) and Sil40 (Fig. 2b), these deformations are much less obvious for Sil60-2 (Fig. 2c) with smaller particle size.

- The $F(R)$ scale is very different from one silica to the other, due to different scattering coefficients. For the same pyrene concentrations, the smallest $F(R)$ values are observed for

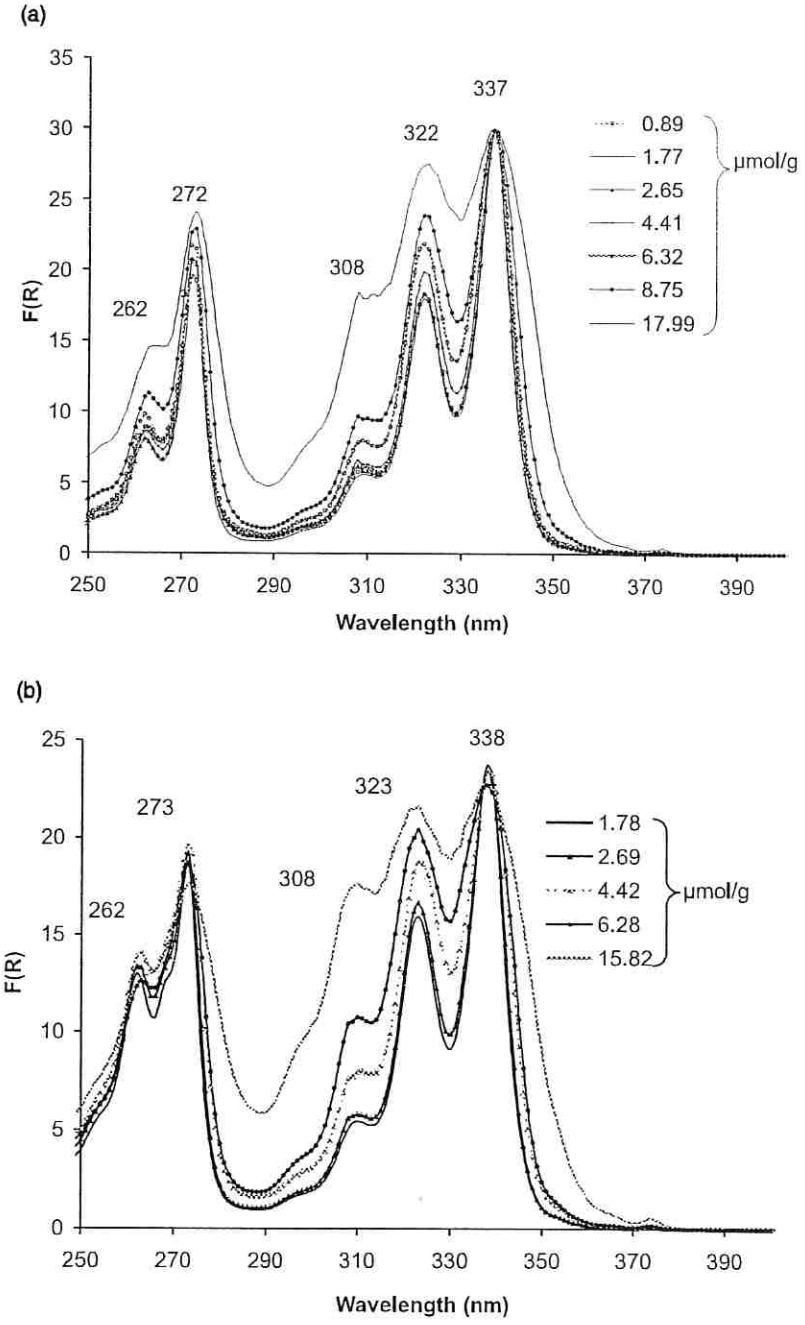

Fig. 2. DRUV spectra of the pyrene derivative **1** adsorbed on different types of silica at different concentrations and normalized on the intensity of the 337 nm band. (a) Sil100, (b) Sil40 and (c) Sil60-2.

Sil60-2 which corresponds to the highest scattering coefficient.

The deformation of the spectra at high concentration may be related to the possible formation of aggregates. These observations are substantiated

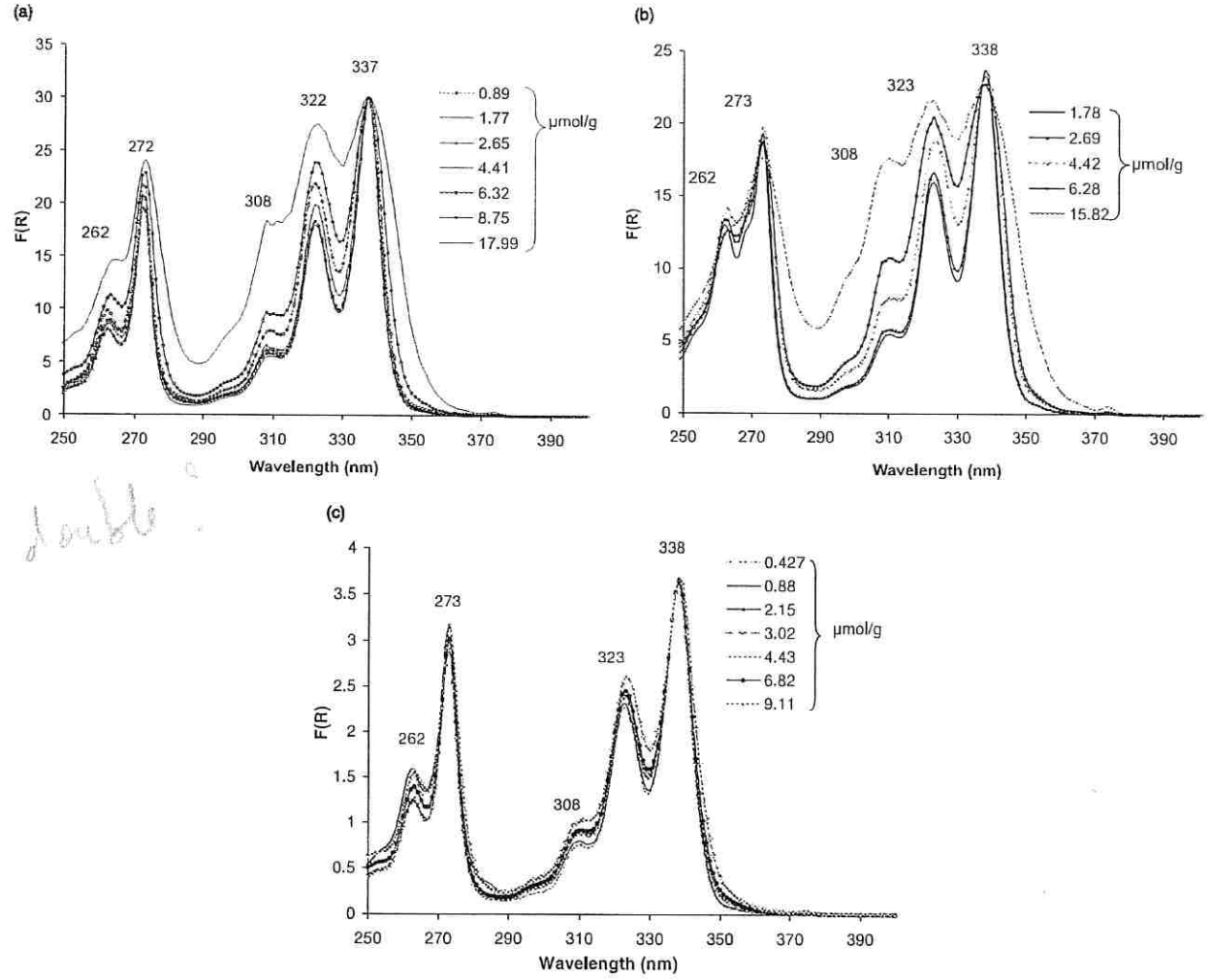

Fig. 2 (*continued*)

by the fluorescence spectra of the powdered adsorbed samples Sil60-1 and Sil60-2 (Fig. 4a and b).

In all spectra, the expected structured emission of monomeric pyrene may be seen between 360 and 425 nm. A structureless emission centered around 470 nm and normally related to excimers is also observed. The excimeric emission is probably the result of the close proximity of molecules adsorbed as aggregates on the surface: this emission will be therefore referred to as "excimer-like" emission [22]. For both silicas, two sets of curves are obtained. For Sil60-1 (Fig. 4a), in the range 0.90–1.75 µmol/g, the amount of aggregates, indicated by the broad featureless "excimer-like" band is small and increases slightly with concentration. In the range 2.7–8.9 µmol/g, excimer formation is more obvious, but its concentration reaches a maximum at 6.2 µmol/g. The same observation still holds true for Sil60-2 (Fig. 4b) but the aggregates emission is only significant after reaching higher concentrations ranges (6.82–9.11 µmol/g). In Fig. 5, the intensities of the excimer band at 472 nm relative to that of the monomer at 375 nm are given for both silicas (black lines), and it appears that excimer formation occurs at a somewhat lower concentration for Sil60-1 than for Sil60-2. In the same figure, the ratio of the relative intensities of the bands at 375 and 394 nm (grey lines) is

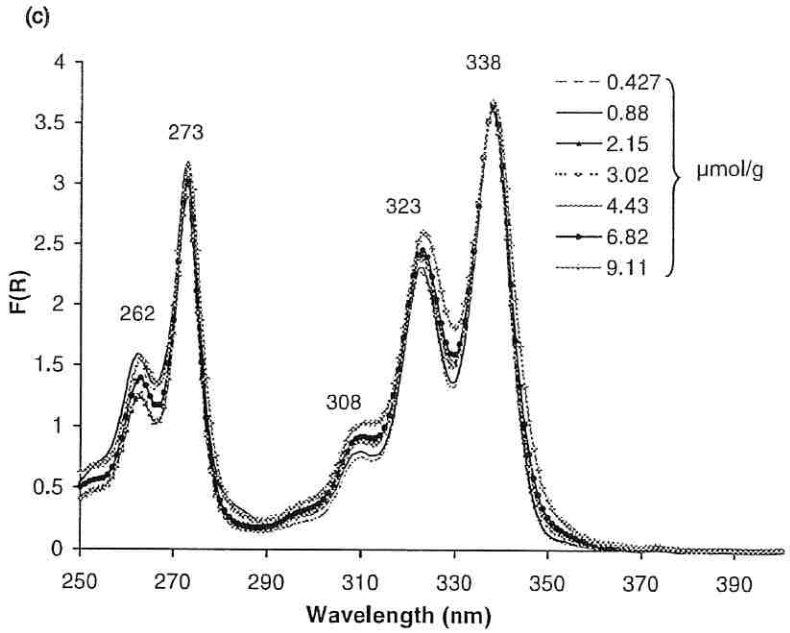

Fig. 2 (*continued*)

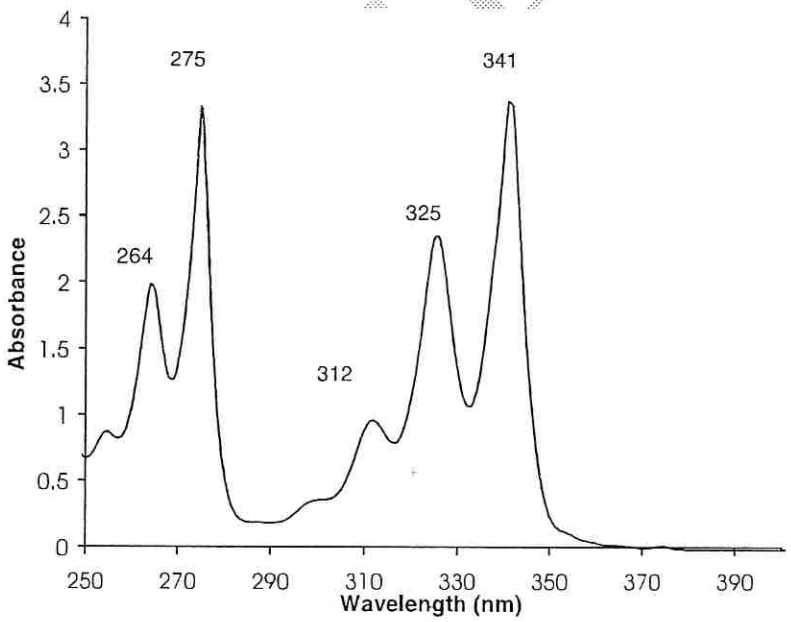

Fig. 3. UV spectrum of the pyrene derivative 1 in CH_3CN solution.

shown to decrease slowly for Sil60-1, while no significant change is recorded for Sil60-2. This ratio is known to decrease when the medium polarity decreases [21,22,30]. Our observations are thus coherent and again indicative of a greater proximity of the pyrene molecules 1 for Sil60-1 than for Sil60-2.

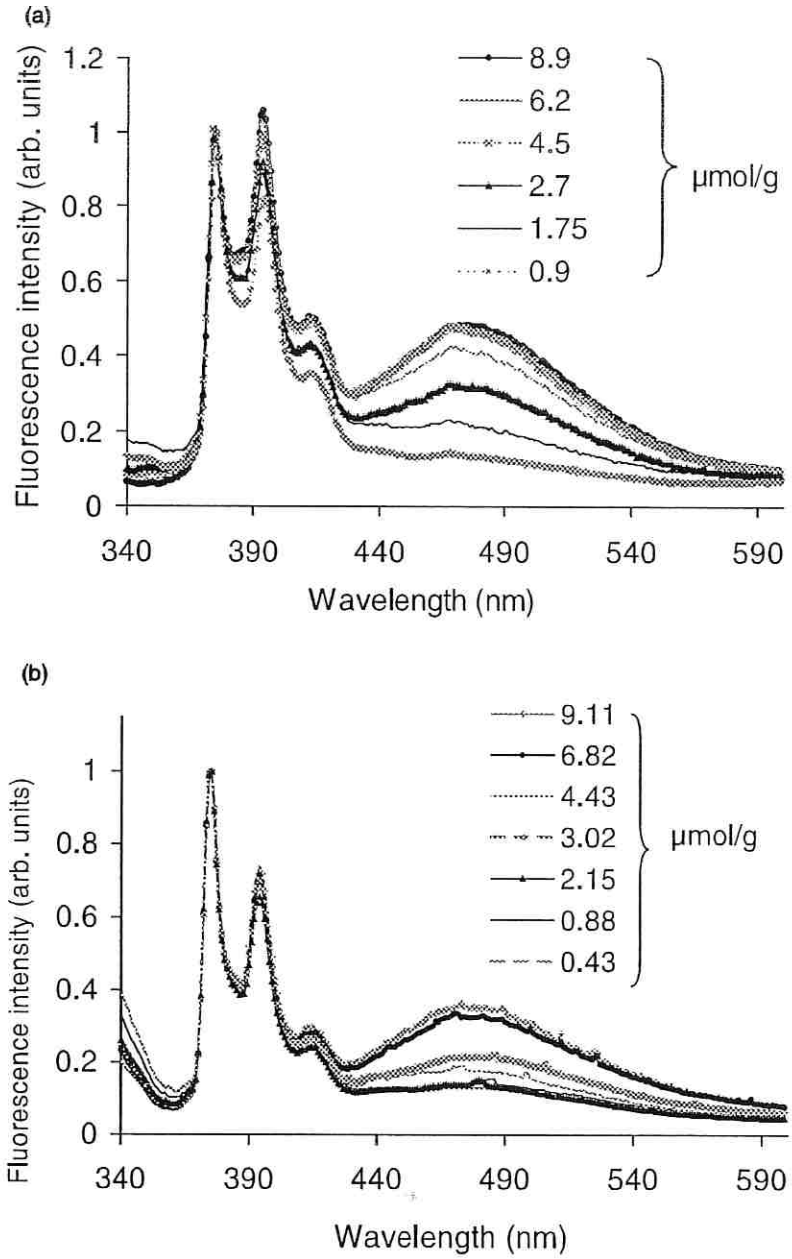

Fig. 4. Normalized fluorescence spectra of the powdered pyrene derivative 1 adsorbed on (a) Sil60-1 and (b) Sil60-2 at different concentrations (λ_{exc}: 340 nm).

To summarize, the UV spectra are indicative of the formation of aggregates in the ground state, while in the same concentration ranges excimer-like emission is rising up in the fluorescence spectra. It probably follows that fluorescent aggregates are formed on the silica surface for concentrations around 2.7 µmol/g for Sil60-1 and 6.82 µmol/g for Sil60-2. In other words, the excimer-like emission is related to the intermolecular ground state association as already observed from fluorescence experiments [31,32].

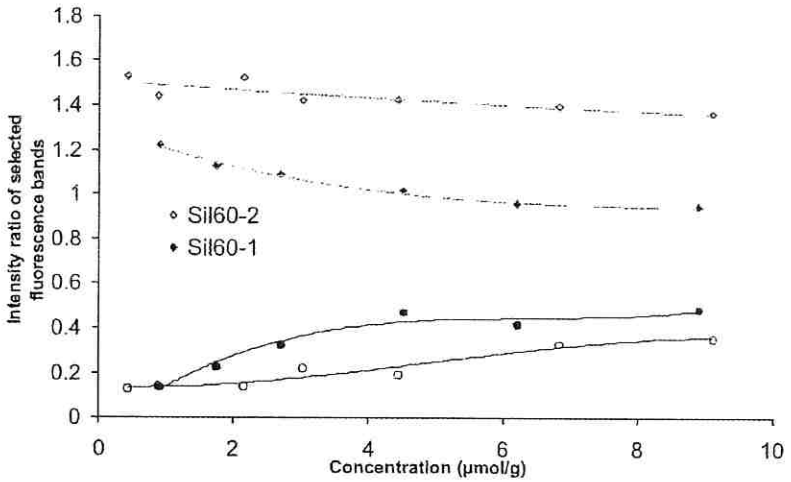

Fig. 5. Relative intensities of the fluorescence bands. (●) I_{472}/I_{375}, (◆) I_{375}/I_{394}.

3.2. Quantitative model of aggregation from DRUV data

As already proposed in the literature [19], a dimerization model may be assumed

$$2M_{ad} \overset{K_D}{\rightleftarrows} (M_2)_{ad} \quad (4)$$

where K_D is an apparent equilibrium constant relating the monomer M_{ad} and the dimer $(M_2)_{ad}$ concentrations. At the solid interface, contrary to solutions, there is no actual equilibrium between adsorbed species. Accordingly K_D should be considered here only as a constant relating monomer and dimer concentrations of adsorbates on the surface.

If C_0 is the initial pyrene derivative concentration, and C_M and C_D the concentrations of the monomer and dimer for a given spectrum, then

$$C_0 = C_M + 2C_D$$
$$F(R) = \varepsilon'_M C_M + \varepsilon'_D C_D$$

According to the dimerization model:

$$K_D = \frac{C_D}{C_M^2}$$

It follows:

$$F(R) = \frac{\varepsilon'_D}{2} C_0 - \frac{2\varepsilon'_M - \varepsilon'_D}{8K_D} + \frac{2\varepsilon'_M - \varepsilon'_D}{8K_D}(1 + 8K_D C_0)^{1/2} \quad (5)$$

with $\varepsilon'_M = \varepsilon_M/S$ and $\varepsilon'_D = \varepsilon_D/S$, the absorptivities (including the scattering coefficient of the given silica) of the monomer and dimer, respectively.

If a first order limited expansion of the square root is applied, i.e. if $8K_D C_0$ is small, then $F(R)$ becomes

$$F(R) = \varepsilon'_M C_0 \quad (6)$$

As expected, it follows that at a given wavelength, the curve giving $F(R)$ versus the concentration should be a straight line passing through the origin at low concentrations and inflecting its shape at higher concentrations.

The whole set of $F(R)$ data at different concentrations for each silica was processed with the Letagrop–Spefo program [25–29], which adjusts the equilibrium constants and the absorptivities. The K_D values was calculated at several wavelengths in the 265–278 and 330–340 nm ranges of high absorptivity. The resulting constants are given in Table 2, and the relative monomer and dimer concentrations deduced from K_D for each silica are displayed in Fig. 6. For the silicas with the same particles size, K_D follows the reverse pore size order, increasing from 4.6×10^4 mol/g for Sil100 to 13×10^4 mol/g for Sil40: the dimer concentration thus increases progressively when the pore size decreases. When comparing the silicas with the same pore size, Sil60-1 (8×10^4 mol/g) and Sil60-2 (1.8×10^4 mol/g), the smallest constant

Table 2
Calculated apparent equilibrium constants K_D (mol/g) and maxima absorption wavelengths of the monomer and dimer of 1 adsorbed on different silicas

Silica	K_D	λ_{max} (nm)	
		Monomer	Dimer
Sil100	4.6×10^4	262, 272, 308, 322, 337	265, 276, 317, 328, 343
Sil60-1	8×10^4	262, 273, 322, 338	268, 279, 316, 329, 344
Sil40	13×10^4	263, 273, 309, 323, 338	266, 277, 318, 331, 344
Sil60-2	1.8×10^4	262, 273, 310, 322, 338	265, 276, 314, 327, 344

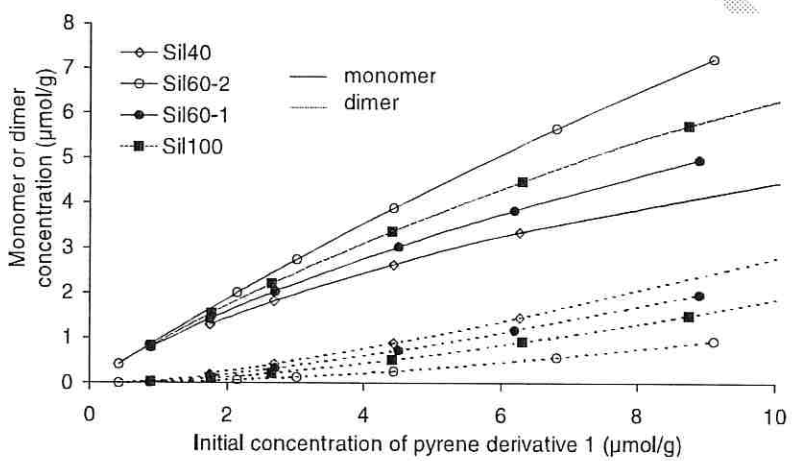

Fig. 6. Relative monomer and dimer concentrations for different silicas at several adsorbate ratios.

is obtained for the silica with the smallest particle size: Sil60-2 presents the lowest ratio of dimer formation among all the silicas studied. From these results, it may be deduced that the dimer concentration is lowest when either a large pore size or a small particle size silica is used.

The obtained absorptivities ε' at each wavelength allow to plot the UV–Visible spectra of both the monomer and the dimer (Fig. 7). It may be noticed that throughout the complete series, the monomer spectra are, as expected, always roughly identical with a very slight hypsochromic shift (Table 2) relative to solution spectra (Fig. 3). As far as the dimers are concerned (Table 2), the absorption maxima wavelengths are all bathochromically shifted versus the monomer. On the other hand, the relative intensities of the dimer bands vary from case to case and, in particular, in the 310 nm range, a broad band noticeably increases when the pore size decreases (Fig. 7a–c). The intensity of this band remains weak for the small particle size silica Sil60-2 (Fig. 7d). It is to be noticed that the obtained dimer spectra are not modified if the highest concentration spectra are omitted in the data processing. This result implies that higher order aggregates are not necessary to explain the observed evolution of the relative intensities of the bands: the dimer model is thus validated.

According to these observations, it may be assumed that different kinds of dimers occur depending on the silica morphology, pore size or particle size. It is well known that two molecules forming an excimer are arranged in parallel or near-parallel pairs [33]. Fujii et al. [32] already reported that relative configurations of neighboring pyrene molecules, depend on the pore size: as the pore size decreases, the dimers tend to have a face-to-face or sandwich configuration. Similarly, our results on Sil100, Sil60-1 and Sil40 with pore sizes of 100, 60 and 40 Å respectively may be ac-

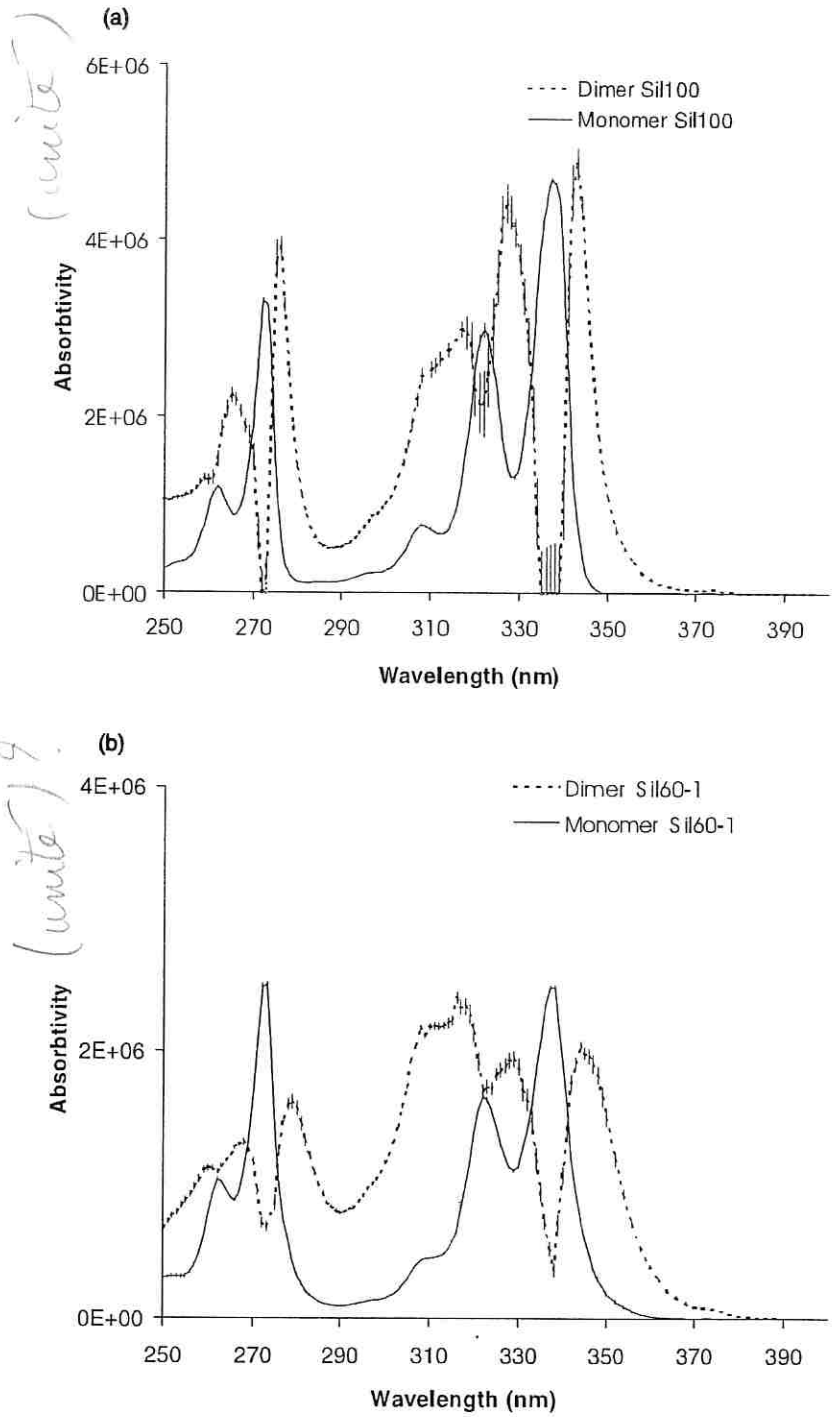

Fig. 7. Calculated UV spectra of the monomer and dimer of **1** on different silicas. Absorptivity $\varepsilon' = \varepsilon/S$ and includes the scattering coefficient S (Eq. (5)). (a) Sil100, (b) Sil60-1, (c) Sil40 and (d) Sil60-2.

counted for by different relative overlapping situations of the pyrene-pairs. For the small particle size Sil60-2, where the aggregates were seen to be formed at higher concentrations, the spectrum

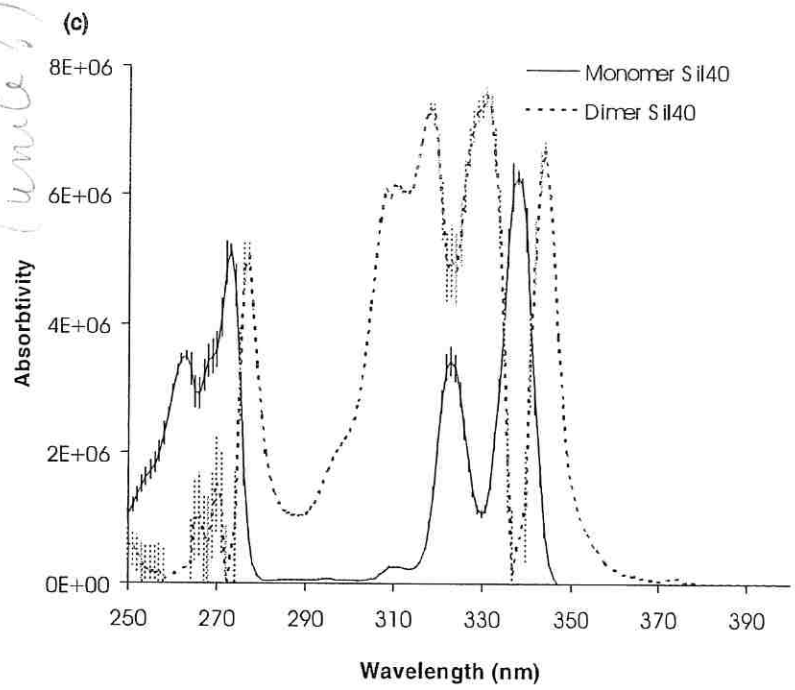

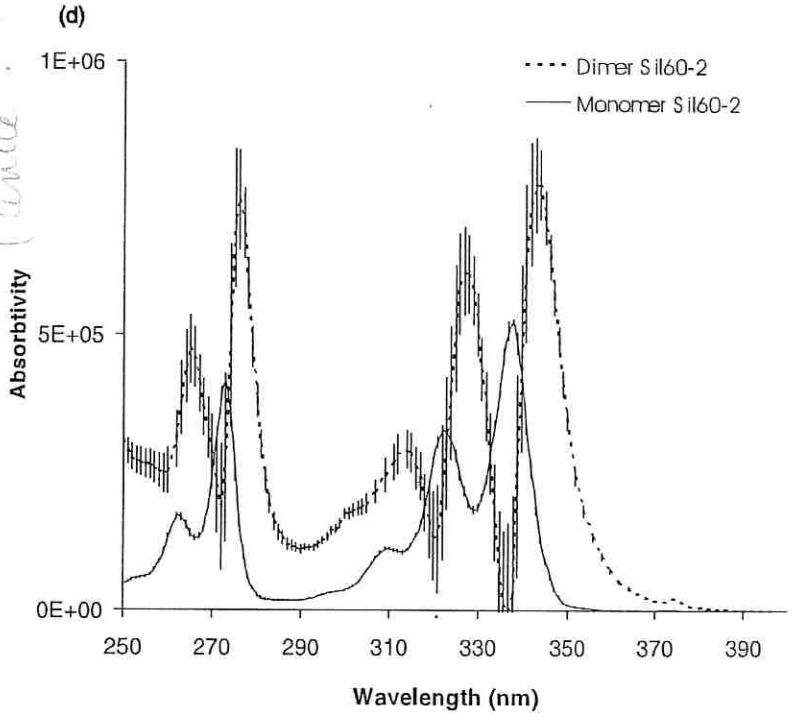

Fig. 7 (*continued*)

distortion is the weakest of the series and only a slight red shift of the spectrum (4–6 nm) is observed relative to that of the monomer (Fig. 7d). This may might indicate that in this case, either the

dimer configuration is no longer face-to-face or that the shift is due to a change in the nature of local adsorption site environment, as for instance a different number of Si–OH per unit area [31] in the Sil60-2 (Fluka) relative to the other silicas (Aldrich). On the other hand, for the small pore size silicas Sil60-1 and Sil40, the enhanced intensity of the 310–318 nm band may be related to the formation of type H (face to face or sandwich) aggregates [19]. In any case, Sil60-2 should be obviously preferred in order to avoid aggregates formation.

3.3. Quantitative determination of 1 grafted on different silicas

The experimental points giving $F(R)$ versus the concentrations for the different silicas used for the calibration have been fitted according to Eq. (5) at three maximum absorption wavelengths: 273, 323 and 338 nm (Fig. 8 at 337 nm for example). It may be noticed that the fit can be used over a large concentration range for Sil60-1 and Sil60-2, as $F(R)$ only smoothly increases with the concentration. However, for Sil100 and Sil40, $F(R)$ becomes too large at about 10 μmol/g so that accurate measurements are no longer possible. All the experimental points are correctly fitted, the largest deviation from the calculated curves being observed for Sil-100. As expected from the model, all curves obtained show a limited linear part at low concentration (below 3 μmol/g except Sil60-2 for which the curve is linear up to 7 μmol/g) and a deviation from linearity at higher concentration.

These fitted curves can be used on the whole concentration range to evaluate grafted silicas provided that the spectra of adsorbed or grafted compounds are similar. The spectra of the grafted silicas compared to those of selected adsorbed silicas are displayed in Fig. 9. The grafted silicas are noted with a letter G in the following to distinguish them from adsorbed silicas. For the G1 series, i.e. grafted silicas at low concentration, the $F(R)$ spectra are nearly identical to those of adsorbed silicas at similar concentrations. This implies similar host-guest interactions in both cases and accordingly, the determination of the loading of the grafted silicas can be deduced from the calibration curves (Fig. 8) obtained for the adsorbed samples. For the G2 series (high concentration grafted silicas), the comparison between $F(R)$ spectra of adsorbed and grafted samples in the same concentration range only holds true for Sil100 (Fig. 9b) and Sil60-2 (Fig. 9d). On the contrary, the spectra of Sil40 G2 (Fig. 9a) and Sil60-1 G2 (Fig. 9c) obviously deviate from those of the adsorbed samples. The fluorescence spectra of all these high concentration samples are roughly similar to those of the adsorbed samples, showing high ratio of excimer-like emission around 470 nm,

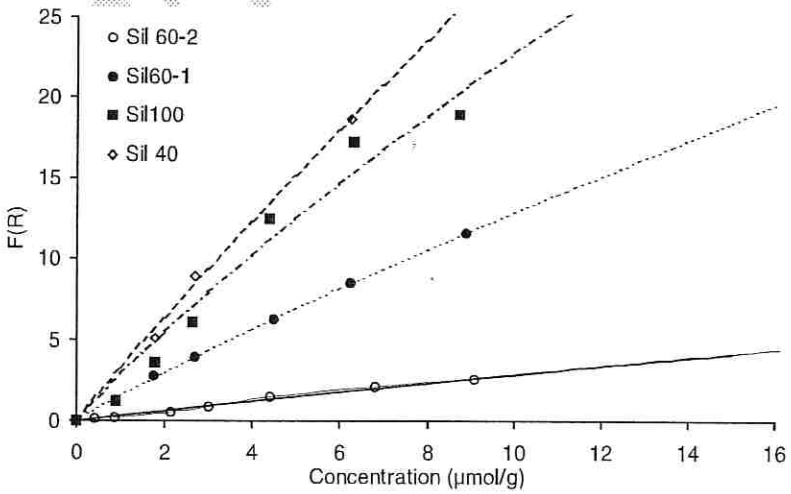

Fig. 8. Experimental points and fitted curves giving $F(R)$ versus the concentrations of adsorbed 1 for different silicas at 337 nm.

except Sil60-1 G2 for which the maximum of the excimer-like emission is shifted to 490 nm. In the case of Sil40 G2 and Sil60-1 G2, this may reflect different host-guest interactions and/or, for these high concentrations, different degrees of aggregation. Alternatively, some hydrolysis and polymerization reaction of **1** during the grafting step, leading to the formation of polymeric species on the surface could account for these deviations, especially for Sil60-1 G2. In these two latter cases, it is excluded to obtain a consistent determination of the loading from the DRUV calibration curves presented previously. Accordingly, the grafting yields for Sil40 G2 and Sil60-1 G2 have been thrown out in the following.

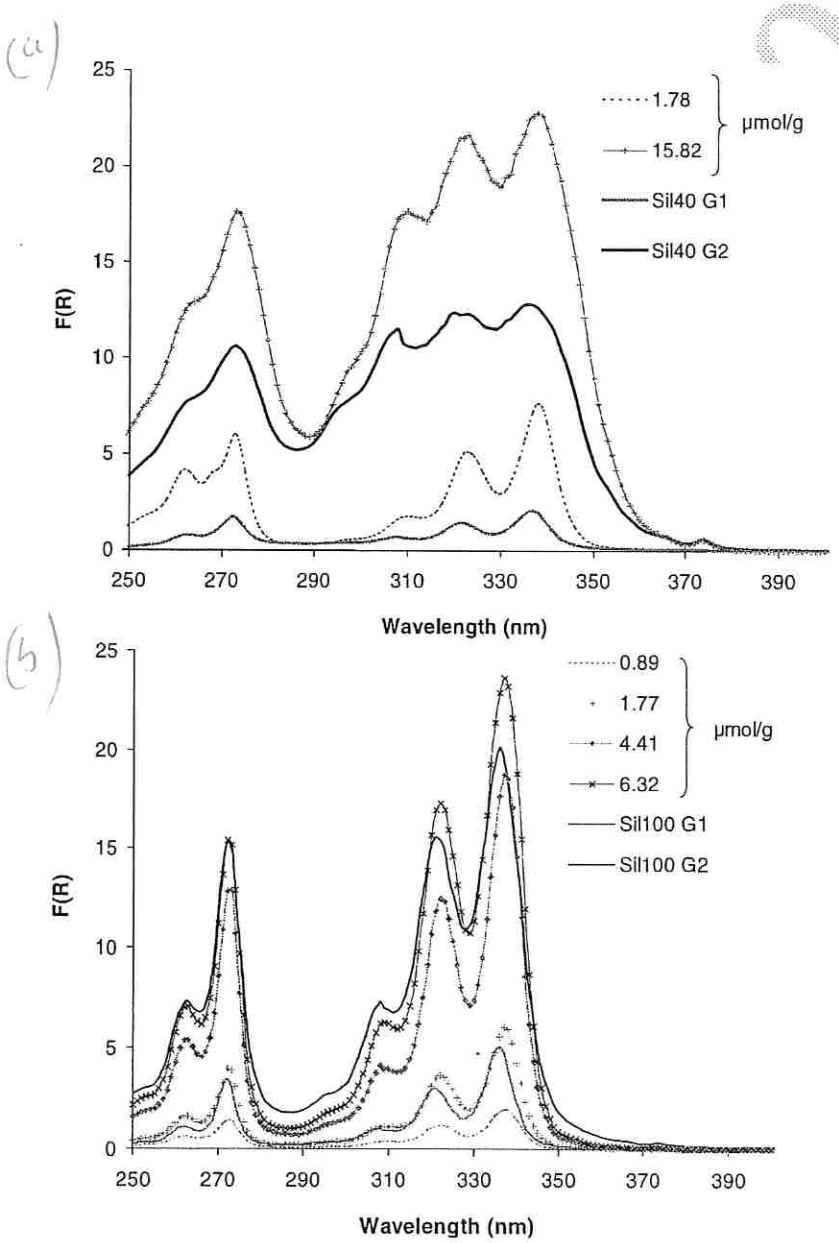

Fig. 9. DRUV spectra of the pyrene derivative **1** grafted on silica compared to spectra of **1** adsorbed on silica at selected concentrations: (a) Sil100, (b) Sil40, (c) Sil60-1 and (d) Sil60-2.

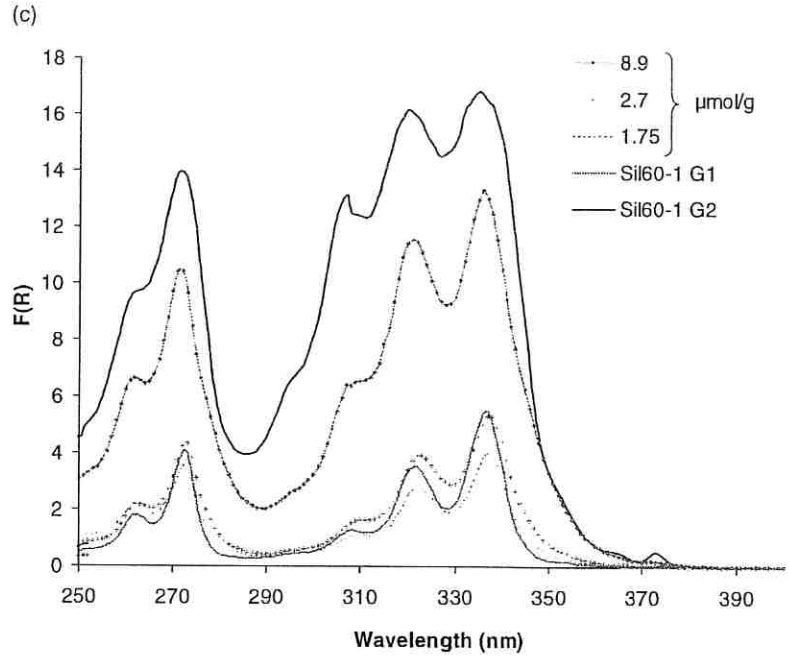

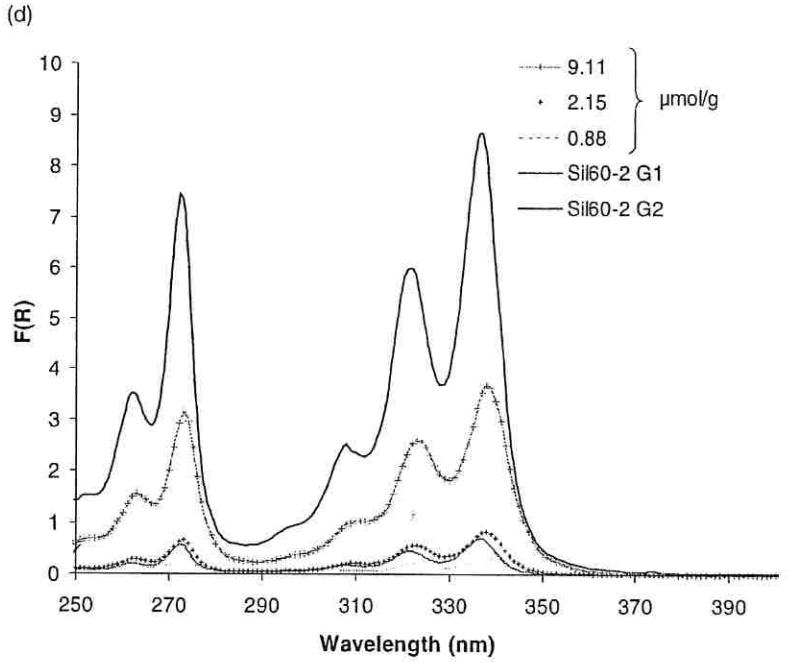

Fig. 9 (*continued*)

For all the other grafted samples, a quantitative determination has been made at each wavelength already used for the calibration procedure (273, 323 and 338 nm). The results are displayed in Table 3 together with the concentrations of **1** introduced in the solvent for the grafting step [22].

Table 3
Calculation of the grafting yields of pyrene derivative 1 on different silicas, using Eq. (5)

Reference of the silica	Pyrene 1[a] (μmol/g)	$F(R)_{323}$	Pyrene 1[b] (μmol/g) (323)	$F(R)_{337}$	Pyrene 1[b] (μmol/g) (337)	$F(R)_{273}$	Pyrene 1[b] (μmol/g) (273)	Grafting yields
Sil100 G1	2.6	2.95	1.0	4.97	1.2	2.97	1.0	41 ± 4
Sil100 G2	25	15.20	6.3	19.67	5.8	15.34	6.7	25 ± 2
Sil60-1 G1	3.0	3.51	2.4	5.46	2.9	4.08	2.0	80 ± 15
Sil40 G1	2.7	1.35	0.4	1.98	0.3	1.71	0.4	14 ± 2
Sil60-2 G1	2.4	0.45	1.4	0.72	1.4	0.57	1.4	60
Sil60-2 G2	24.5	5.73	21.6	8.13	23.8	7.43	23.7	93 ± 4

[a] Concentration of pyrene 1 used in the grafting process.
[b] Concentration of pyrene 1 calculated with measurements at the indicated wavelength (nm).

Except for the cases of Sil60-1 G1, the confidence limits for the calculated grafting yields are found to be below 8%.

In the case of Sil-100, the grafting yields decrease from 41% to 25% (1.1 and 6.3 μmol/g of grafted 1 for Sil100 G1 and Sil100 G2 respectively) in spite of the fact that the concentration of 1 has been increased, owing to the saturation of the grafting sites on silica.

High grafting yields are obtained for Sil60. For Sil60-1 G1, the results vary significantly between the three considered wavelengths (2.0–2.9 μmol/g for Sil60-1 G1). This inaccuracy is related to the slight deviation of the spectrum of the grafted compound relative to those of adsorbed ones (Fig. 9c). In the case of Sil60-2, the highest grafting yield is obtained for the highest concentration of 1, indicating that the surface silanols are not saturated even at high concentration.

Finally, for grafted Sil-40 G1 the amount of grafted 1 is 0.4 μmol/g corresponding to a very low grafting yield (14%).

No clear-cut explanation can be given to account for the results on Sil60-1 G2 and Sil40 G2: is the deviation related to higher-order aggregates or to hydrolysis and polymerization reactions of 1 before grafting? Some preliminary results indicate that the adsorbed triethoxysilyl derivative 1 can be covalently grafted spontaneously at room temperature. Under these mild conditions, hydrolysis and polymerization reactions of 1 before grafting are thus unlikely. If this can be confirmed, a better control of the loading might be possible since calibration and grafting should be run under similar conditions. Further experiments are being carried out to verify this proposal.

In any case, the DRUV spectroscopy appears as a very useful tool to assess qualitatively and quantitatively organic adsorbates on silica, especially in low concentration domains where other more usual methods are rather inaccurate.

4. Conclusions

This study further confirms that DRUV is a powerful technique to evidence qualitatively the interactions between molecules adsorbed on an inert substrate like silica. This work moreover demonstrates that a quantitative treatment of the data is also possible even at high concentrations, provided that the sampling methods and recording conditions are carefully controlled. By extension of a well known processing of the spectrophotometric data in solution, the relative dimer and monomer concentrations as well as their respective spectrum in the adsorbed state may be derived.

This set of results yields a calibration curve giving $F(R)$ versus the concentration of adsorbed species, against which the signals of the same species grafted on silica can be evaluated. Grafting ratios, hardly obtained by other techniques, are thus available and the method appears especially sensitive at low or very low loading.

These results also give some indications for future uses of grafted photosensitizers in photochemical applications. A silica with small particle size or large pore size should be preferred to avoid excimer formation. Furthermore, in order to use

the DRUV determination method, small particle size silica offers an additional advantage such as a reduced $F(R)$ scale owing to a large scattering coefficient.

Finally, the general grafting method used in this study leads to poorly controlled loading at high concentration. In some cases, unexplained deformation of the spectra relative to those of adsorbed samples are observed. Some improvement in the synthetic method is thus under investigation.

Acknowledgements

The author gratefully acknowledge NATO for financial support for this collaborative research.

References

[1] A. Cauvel, G. Renard, D. Brunel, J. Org. Chem. 62 (1997) 749–751.
[2] Julliard M, in: M. Chanon (Ed.), Homogeneous Photocatalysis, Wiley, London, 1997, pp. 222–261.
[3] H. Okabayashi, I. Shimizu, E. Nishio, C.J. O'Connor, Colloid Polym. Sci. 275 (1997) 744–753.
[4] L. Horner, J. Klaus, Liebigs Ann. Chem. (1981) 792–810.
[5] D. Derouet, S. Forgeard, J.C. Brosse, J. Emery, Y. Buzares, J. Polym. Sci. 36 (1998) 437–453.
[6] A.M. Nechifor, A.P. Philipse, F. de Jong, J.P.M. van Duynhoven, R.J.M. Egberink, D.N. Reinhoudt, Langmuir 12 (1996) 3844–3854.
[7] R.S.S. Murthy, D.E. Leyden, Anal. Chem. 58 (1986) 1228–1233.
[8] F. Boroumand, H. van den Bergh, H. Moser, J. Anal. Chem. 66 (1994) 2260–2266.
[9] E. Pere, H. Cardy, O. Cairon, M. Simon, S. Lacombe, J. Vib. Spectrosc. 25 (2001) 163–175.
[10] B.M. Weckhuisen, A. Bensalem, R.A. Schoonheiydt, J. Chem. Soc. Faraday Trans. 94 (1998) 2011–2014.
[11] B.M. Weckhuisen, A.A. Verberckmoes, J. Debaere, K. Ooms, I. Langhans, R.A. Schoonheiydt, J. Mol. Catal. A: Chem. 151 (2000) 115–131.
[12] A. Di Paola, L. Palmisano, A.M. Venezia, V. Augugliaro, J. Phys. Chem. B 103 (1999) 8236–8244.
[13] X. Gao, M. Banares, I. Wachs, J. Catal. 188 (1999) 325–331.
[14] D. Trong On, L. Le Noc, L. Bonneviot, Chem. Commun. 3 (1996) 299–300.
[15] S. Dzwigaj, M. Matsuoka, R. Franck, M. Anpo, M. Che, J. Phys. Chem. B 102 (1198) 6309–6312.
[16] F. Blatter, F. Moreau, H. Frei, J. Phys. Chem. 98 (1994) 13406–13407.
[17] G. Grubert, M. Wark, N.I. Jaeger, G. Shulz-Ekloff, O.P. Tkachenko, J. Phys. Chem. B 102 (1998) 1665–1671.
[18] A.M. Bothelho do Rego, L. Penedo Pereira, M.J. Reis, A.S. Oliveira, L.F. Vieira Ferreira, Langmuir 13 (1997) 6787–6794.
[19] L.F. Vieira Ferreira, A.S. Oliveira, F. Willkinson, D. Worrall, J. Chem. Soc. Faraday Trans. 92 (1996) 1217–1225.
[20] A.A. Christy, O.M. Kvalheim, R.A. Velapoldi, Vib. Spectrosc. 9 (1995) 19–27 and references cited.
[21] K. Kalyanasundaram, J.K. Thomas, J. Am. Chem. Soc. 99 (1977) 2039–2044.
[22] J.L. Habib Jiwan, E. Robert, J.Ph. Soumillion, J. Photochem. Photobiol. A: Chem. 122 (1999) 61–68.
[23] L.F. Vieira Ferreira, J.C. Netto-Ferreira, I.V. Khmelinskii, A.R. Garcia, S.M.B. Costa, Langmuir 11 (1995) 231–236.
[24] L.F. Vieira Ferreira, P.V. Cabral, P. Almeida, A.S. Oliveira, M.J. Reis, A.M. Botelho do Rego, Macromolecules 31 (1998) 3936–3944.
[25] L.G. Sillen, Acta Chem. Scand. 18 (1964) 1085–1098.
[26] L.G. Sillen, B. Warnqvist, Ark. Kemi 31 (1968) 341–351.
[27] R. Anrnek, L.G. Sillen, O. Wahlberg, Ark. Kemi 31 (1968) 353–363.
[28] C. Brauner, L.G. Sillen, R. Whiteker, Ark. Kemi 31 (1968) 365–377.
[29] L.G. Sillen, B. Warnqvist, Ark. Kemi 31 (1968) 377–390.
[30] D.C. Dong, M.A. Winnik, Can. J. Chem. 62 (1984) 2560–2565.
[31] E. Wellner, M. Ottolenhi, D. Avnir, Langmuir 2 (1986) 616–619.
[32] T. Fujii, A. Ishii, N. Takusagawa, H. Yamashita, M. Anpo, J. Photochem. Photobiol. A: Chem. 86 (1995) 219–224.
[33] J.B. Birks, Photophysics of Aromatic Molecules, Wiley, London, 1970, pp. 301–372 (Chapter 7).